Growth, photoluminescence, lifetime, and laser damage threshold studies of 1, 3, 5-triphenylbenzene (TPB) single crystal for scintillation application

Manikandan Murugesan[1] · Rajesh Paulraj[1] · Ramasamy Perumalsamy[1] · Maurya Kamlesh Kumar[2]

Abstract

The 1, 3, 5-triphenylbenzene (TPB) single crystal has been grown using slow cooling seed rotation technique. Optical transmittance of the grown crystal was obtained from UV–Visible analysis. The grown TPB crystal has good transmission in the entire visible region with a lower cutoff wavelength of 330 nm. The solubility of TPB material was determined using toluene as a solvent with different temperatures. The full width at half maximum is 18 arcsec, which indicates that the crystal is of good quality. The TPB crystal was excited (λ_{exc}) at 307 nm, and the corresponding emission (λ_{em}) has been observed at 352 nm. The laser-induced damage threshold (LDT) value of grown crystal is 1.25 GW/cm^2. Third-order nonlinear optical susceptibility $\chi(3)$ is determined using the Z-scan technique as 3.07422×10^{-09} esu. The TPB crystal proves its suitability for scintillation applications and optoelectronic device fabrications.

1 Introduction

The organic materials are having many advantages such as low cost, high optical nonlinearity, low dielectric constant, and fast response time (detection application) compared to the inorganic materials [1–4]. Nonlinear optical materials (NLO) are considered crucial due to their role in the development of technology and its impact on various industries and new potential applications [5, 6]. Organic crystals play a crucial role in different potential applications such as frequency generation, optical fiber communication, and scintillation application. The rapid growth of crystals in a shorter period while maintaining the crystal quality and large size has been a topic of interest for some years now [7–11]. Some of the organic scintillators such as p-terphenyl, anthracene, naphthalene, and stilbene are widely used for fast neutron detection in gamma radiation background due to their more hydrogen content which allows for detecting the neutron when proton recoils [12]. The 1, 3, 5-triphenylbenzene (TPB) single crystal is one of the organic scintillator materials for high-energy neutron detection applications, which gives good pulse shape discrimination, and also TPB is an attractive material compared to stilbene for detection application [13].

There are numerous methods to grow organic crystals, mostly solution, and melt growth methods. In the solution growth method, some organic materials face solvent inclusion problem and it leads to decrease the optical quality of the crystals. The growth of TPB crystals using solution was reported in several papers [14, 15]. Nonlinear optical property has been investigated in many organic materials [4, 5, 9, 11]. In this paper, we are interested to improve the quality and size of the crystal by using a slow cooling seed rotation method. This technique is suitable to grow defect-free and large-size crystal from the solution [16]. Good-quality single crystals are essential to designing innovative devices such as semiconductor devices and photonic devices which are used for carrying the information, telecommunications, and laser applications [5, 17]. The laser damage threshold measurements were taken for evaluating the quality of the crystal for laser applications. The device

✉ Rajesh Paulraj
  rajeshp@ssn.edu.in

1 Centre for Crystal Growth, Department of Physics, SSN College of Engineering, Kalavakkam, Tamilnadu 603110, India
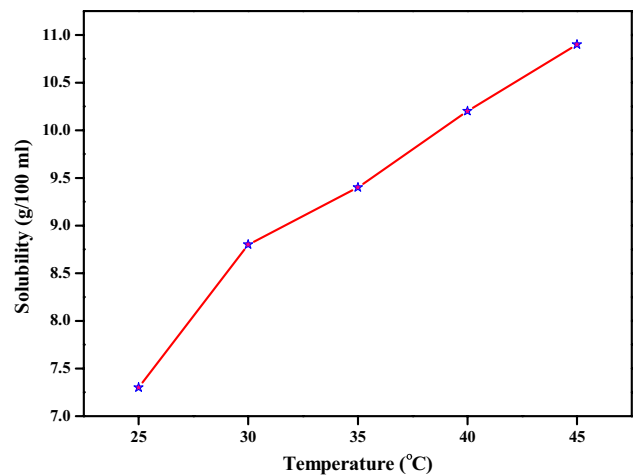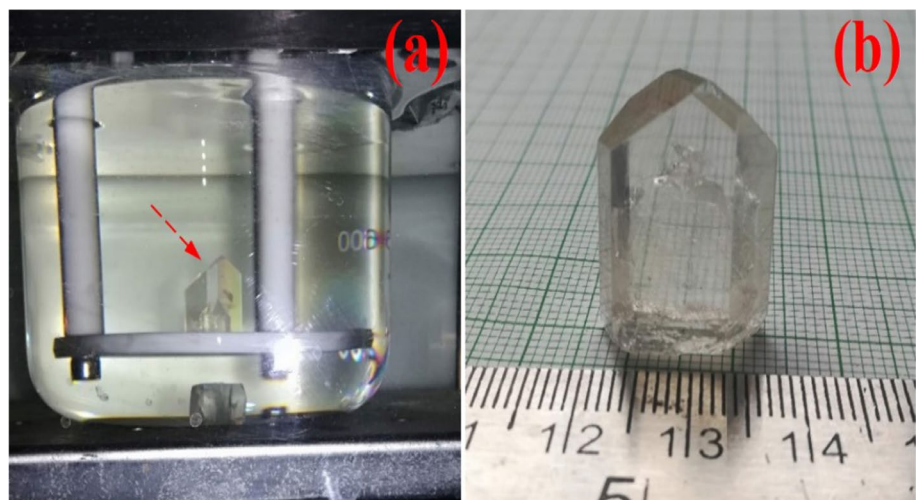
2 Crystal Growth and X-Ray Analysis Division, CSIR-National Physical Laboratory, New Delhi 110012, India

fabrication of high-tech laser devices mainly depends on the high-efficient nonlinear optical (NLO) single crystals that determine the excellent linear and nonlinear characteristics of the materials. The nonlinear absorption coefficient (β) and the refractive index are essential parameters in determining the suitability for device applications. Furthermore, the present paper discusses the growth, structural, optical, third-order nonlinear optical and various other properties of the grown TPB crystals.

2 Crystal growth: slow cooling method

TPB crystals were grown from aqueous solution by slow cooling seed rotation method. This apparatus consists of a seed rotation controller coupled with a stepper motor, which is controlled using a microcontroller-based drive. Initially, the TPB powder was dissolved using a toluene solvent. The solution was continuously stirred for 6 h to maintain homogeneity for crystal growth. A good-quality seed crystal of size $3 \times 3 \times 5$ mm^3 was fixed at the center of the crystallizer. The applied rotation speed was 30 rpm. The crystal growth was carried out in a 2000-mL standard crystallizer. In total, 1600 mL saturation solution of TPB was prepared and the saturation temperature was 40 ℃. The solution was filtered by the Whatman filter paper of pore size 11 μm. After filtration, the temperature of the solution was increased to 50 ℃ for about 24 h. Then the temperature was reduced to the saturation temperature (40 ℃) in steps of 1 ℃ per hour. The saturation solution of TPB was kept inside a constant temperature bath. From the saturation point (40 ℃), the temperature was decreased at the rate of 0.10 ℃ per day. After a period of 30-day growth, good-quality crystals were harvested. The grown TPB crystal is shown in Fig. 1.

Fig. 2 Solubility of TPB using toluene as solvent

3 Results and discussion

3.1 Solubility

To grow a large-size and good-quality crystal, solubility plays an important role in low-temperature slow evaporation solution growth method. The size of the crystal depends on the amount of the material available in the solution for the growth, which decides the solubility of the material in that appropriate solvent and temperature of the solution. The solubility of TPB single crystal has been determined using toluene as a solvent in the temperature range 25–45 ℃ with a 5 ℃ interval. The solubility experiment was carried out in a constant temperature water bath with a cryostat facility. The amount of compound required for making the saturated solution at different temperatures and solubility of TPB is estimated gravimetrically, and the

Fig. 1 a Growing crystal inside the constant temperature water bath. **b** Grown TPB crystal

obtained solubility curve is shown in Fig. 2. It shows that the concentration of the solution is increasing with the increase in temperature.

3.2 Single-crystal and powder XRD analysis

The single-crystal XRD data of grown TPB crystals were recorded using Bruker axes SMART APEXII single-crystal XRD instrument with monochromatic MoKα radiation at room temperature to determine cell parameters. The XRD data show that TPB crystal belongs to the orthorhombic structure and the lattice parameters are $a = 7.43$ Å, $b = 19.72$ Å, $c = 11.12$ Å, $\alpha = \beta = \gamma = 90^{\circ}$ and volume is 1685 Å^3 [14]. The powder form of the TPB single crystal was taken for the powder X-ray diffraction analysis using the Empyrean PANalytical diffractometer using nickel-filtered Cu–Kα radiation (0.15418 nm) as a source and operated at 40 kV. The sample was scanned for the range (2θ) between 5° and 60° at room temperature. The powder X-ray diffraction pattern of the grown crystal with the 2θ values indexed using the 'TWOTHETA' software is shown in Fig. 3. Powder XRD results show the good crystalline nature of the grown crystal.

3.3 FTIR analysis

The different functional groups present in the grown crystal were identified by FTIR spectral analysis. FTIR spectrum was recorded using Bruker AXS FTIR spectrometer in the range from 4000 to 500 cm^{-1} with ATR mode. The FTIR spectrum is shown in Fig. 4. The aromatic rings in a structure are typically determined from the C–H and C=C–C ring-related vibrations. The bands are defined by the number and positions of the C–H and C=C–C bonds around the ring
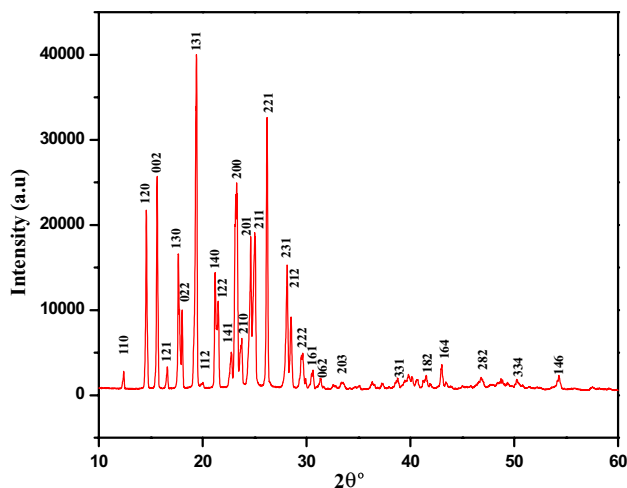

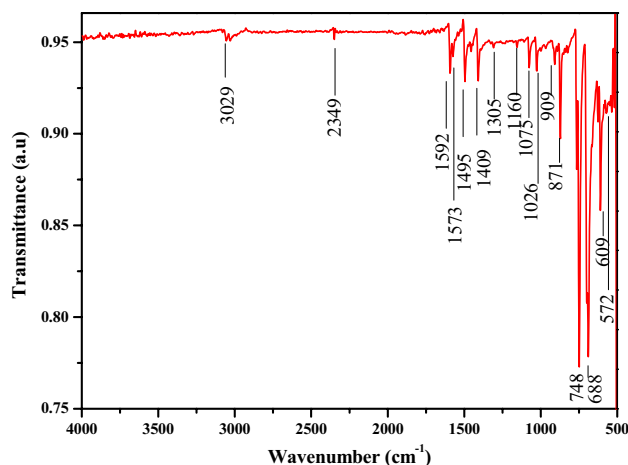**Fig. 3** Powder XRD of TPB crystal

Fig. 4 FTIR spectrum of TPB crystal

in the title compound. The strongest absorptions for aromatic compounds that occur in the range between 900 and 650 cm^{-1} are due to the C-H vibrations out of the plane of the aromatic ring [18]. The absorption band at 3029 cm^{-1} is corresponding to the C–H stretching vibration. The C=C–C aromatic ring stretching vibrations occur at 1594, 1573, and 1495 cm^{-1}. The aromatic C–H in-plane bending vibrations appeared at 1160, 1075, and 1026 cm^{-1}, and aromatic C–H out-of-plane bending vibrations occurred at 909 and 871 cm^{-1} [19]. The C–C and C=C stretching vibrations of benzene rings generally occur in the range from 1650 to 1400 cm^{-1} [20]. The C–C stretching vibrations have been observed at 1592, 1573, 1495, and 1409 cm^{-1}, and C–C bending modes are observed at 609 and 572 cm^{-1}. Generally, 1, 3, 5-trisubstituted benzenes have strong absorption at 865–810 and lesser intensity bands at 730–660 cm^{-1}. The absorption band at 748 and 688 cm^{-1} was assigned monosubstitution of phenyl groups [21].

3.4 UV–Vis analysis

The UV–Vis analysis was used to determine the transmittance spectrum. The lower cutoff wavelength and good transmittance in the entire visible regions are very important parameters for materials to be used for laser and optical device applications [8, 22]. The crystalline defects affect the optical properties, for instance, light absorption and refractive index. The optical transmittance spectrum of the grown TPB crystal with 2 mm thickness has been recorded using PerkinElmer UV–Vis–NIR Spectrophotometer with the range between 200 and 1100 nm. The recorded transmittance spectrum is shown in Fig. 5. The cutoff wavelength (λ_{cutoff}) of the grown crystal is found to be 330 nm. The spectrum indicates that the present TPB crystal has good optical transmission compared to the earlier reports [15, 23], which
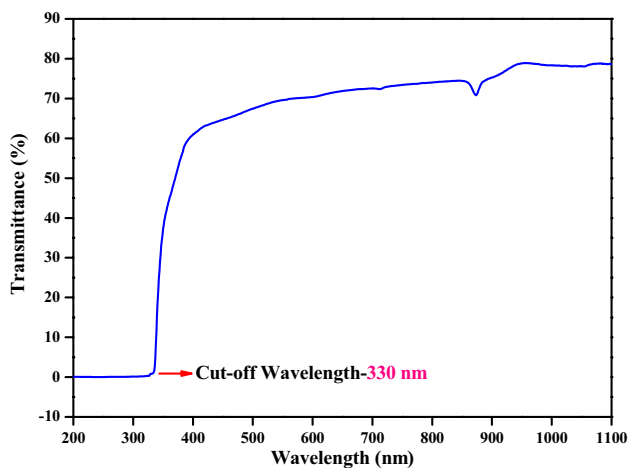
Fig. 5 Transmittance spectrum of TPB crystal

is an appropriate asset for NLO activity and which makes it suitable to be used in the optical application for SHG laser radiation applications [24].

3.5 Photoluminescence and lifetime analysis

The photoluminescence (PL) emission of the material may find various potential applications such as detection applications. Photoluminescence analysis is a noncontact, nondestructive technique of probing the electronic structure of materials. In principle, when the light (photons) is directed onto a sample, it absorbs photons and then emits them at different wavelengths, and the resultant light can be dispersed. Generally, the aromatic molecules contain multiple conjugated bonds which lead to a high degree of resonance stability. The emission spectrum of the grown crystal was examined through photoluminescence (PL) spectral analysis. The PL analysis of TPB single crystal was carried out using the Shimadzu Spectrofluoro photometer RF-5031 PC series with a slit width of 3 nm at room temperature.

The emission spectrum was measured in the range between 300 and 500 nm and only one violet emission band with a peak wavelength at 352 nm was observed, which is due to $\pi^*-\pi$ electron transition in the phenyl ring. The emission spectrum of the TPB crystal is shown in Fig. 6. Such a strong peak indicates that grown TPB crystal contains good crystallinity and low crystalline defects. An important feature of the organic scintillator for detector application is to exhibit various lifetime at the same emission wavelength [13]. The decay time curves are well fitted with the following function.

$$R(t) = B_1 e^{\frac{-t}{\tau 1}} + B_2 e^{\frac{-t}{\tau 2}} \tag{1}$$
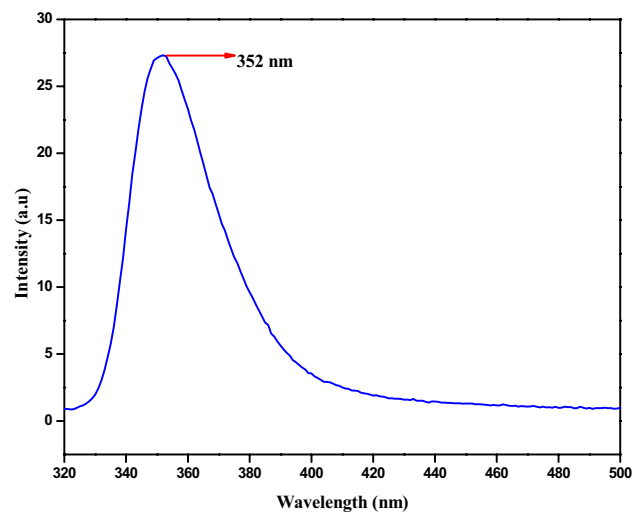

Fig. 6 PL spectrum of TPB crystal

where B_1 (06.85) and B_2 (98.35) are amplitudes of prompt and delayed emissions, respectively, and τ_1 and τ_2 are lifetimes. The fast scintillation decay time in the organic crystal is generally 2 to 30 ns. The grown TPB crystal exhibits 12 ns (τ_1) and 30 ns (τ_2), and it is well matched compared to earlier reported values [13, 15]. The decay time of grown TPB crystal is shown in Fig. 7. The prompt (τ_1) and delayed (τ_2) lifetimes are corresponded to de-excitation of singlet energy-level transition and delayed emission due to collisional interaction pairs of molecules in the lowest excited triplet energy state, respectively [25].

3.6 High-resolution X-Ray diffraction analysis

High-resolution X-ray diffraction analysis shows the crystalline perfection of the grown crystal. The crystalline perfection of the grown crystal indicates its suitability for device
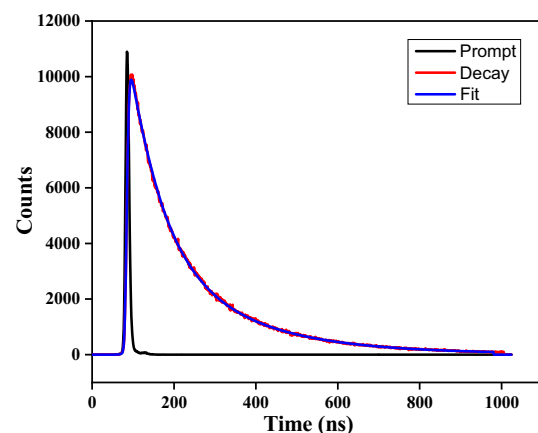

Fig. 7 Decay curve of TPB crystal

fabrication [26]. When increasing the crystalline perfection of crystal, it is possible to enhance the various properties [10]. A high-resolution diffraction curve (DC) was recorded for the crystals grown using the slow cooling method. A monochromatic Mo $K\alpha_1$ beam from the three monochromator Si crystals at dispersive $(+,-,-,+)$ configuration was used for analysis. The crystals are aligned in $(+,-,-,+)$ configuration. The specimen surface was lapped and polished by water before subjecting to the recording. This reveals the single peak formation, indicating the crystal under study is free from structural grain boundaries. Observation shows the symmetry of the DC with respect to the peak position denoted by the dotted lines in the figure, and it indicates an ideally perfect crystal with good quality. A single sharp DC with very low FWHM of the curve is 18 arcsec which indicates good perfection of grown TPB crystal from the plane wave theory of dynamical X-ray diffraction [27], and the spectrum is shown in Fig. 8.

3.7 Laser damage threshold studies

The laser damage study of the crystals is extremely important since it limits their performance in NLO applications [28]. Laser damage threshold (LDT) is the ability limit of material to withstand intense laser irradiation without observable changes in its optical properties. The LDT of an optical crystal is an important factor affecting its applications. The higher LDT value of materials is the most important property for the device fabrications. If the materials are having a low LDT value, it is not suitable for many applications. LDT values depend on many factors such as laser pulse width, wavelength, spatial profile pulse, quality of the crystal surface, type of modes and defects in the sample [29].

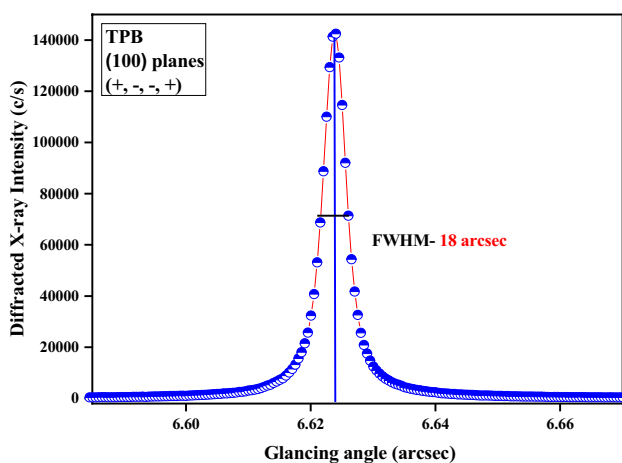Generally, the laser damage threshold (LDT) experiment is measured by the two-mode process: (i) single-shot mode and (ii) multiple-shot mode. LDT experiment was carried out in single-shot mode using a Q-switched Nd: YAG laser generating nanosecond pulses at 532 nm (second harmonic of the fundamental wavelength at 1064 nm). The cut and polished good-quality TPB single crystals were used for the LDT measurement, and the crystal thickness is 2 mm. The incident energy (milli-Joule) was applied to TPB single crystal, and the output of the incident laser beam was measured using an attenuator. The focal length of the plano-convex lens is observed at 10 cm, and it could be attached by the translation stage of the sample holder. Initially, 10 mJ of energy was applied for the crystal, and no damage was observed. When the energy is increased beyond 10 mJ, a spot is observed in the crystal. At 50 mJ, a crack was observed on the surface of the grown crystal. The laser damage pattern of the grown crystal is shown in Fig. 9. The LDT (power density) value of the grown crystal was calculated using the following expression.

$$\text{Power Density } \left(P_d\right) = \frac{E}{\tau\pi(\omega_Z)^2} \tag{2}$$

where E is the input energy (milli-Joule), τ is the pulse width (ns), and ω_z is the radius of the spot size (mm) in the focused beam on the crystal. The laser damage threshold value of grown crystal was found to be 1.251 Gw/cm^2. The laser damage threshold value of TPB material is higher compared to several organic and inorganic materials [30–32].

3.8 Third-order nonlinear optical analysis (Z-scan)

The Z-scan measurement is widely used to measure the nonlinearity of materials, such as intensity-dependent
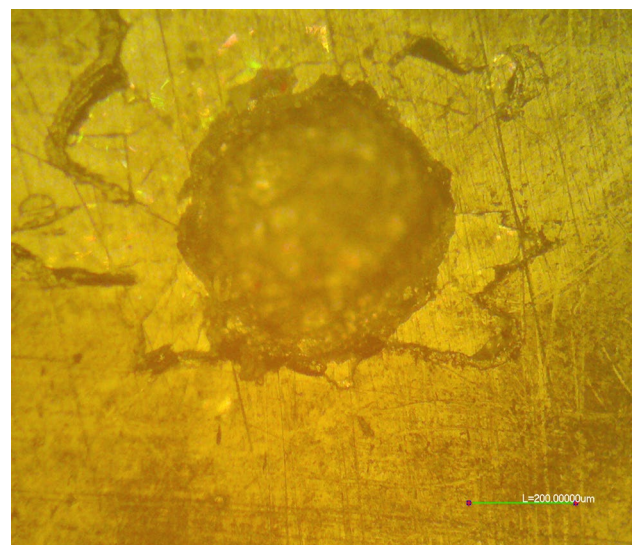
Fig. 8 High-resolution diffraction curve for TPB single crystal

Fig. 9 Laser damage pattern of the grown TPB crystal

nonlinear refractive index, absorption coefficient and third-order nonlinear optical susceptibility (χ3) [33–37]. This measurement is important to find out the crystalline perfection. The nonlinear optical properties can be measured by the Z-scan technique (open aperture (OA) and closed aperture (CA) configurations). This measurement, 532-nm laser wavelength (semiconductor–continuous-wave laser) and 10 mW power, was used. The optical path length is 675 mm. The beam radius at the aperture and radius of aperture are 20 mm and 3 mm, respectively. Laser power I_o is 3.47 kW/cm^2, and the focal length of the lens is 103 mm. Generally, the nonlinear optical absorption could be classified into two categories, such as saturable absorption (SA) and reverse saturable absorption (RSA). The transmittance of the sample increasing with increasing intensity is called saturable absorption, and the transmittance decreasing with increasing intensity is called reverse saturable absorption [30]. For open aperture (OA) Z-scan mode, a lens collects the entire laser beam transmitted through the sample and the open aperture gives information about the nonlinear absorption coefficient [35]. The difference between the normalized peak and valley transmission (ΔTp–v) is calculated from the equation given below:

$$\Delta T_{p-v} = 0.406(1 - S)^{0.25}|\nabla\phi| \tag{3}$$

where $|\Delta\phi|$ is on-axis phase shift on the focus, S is the linear transmittance of the aperture, and it was estimated by:

$$S = 1 - \exp\left(\frac{-2r_a^2}{\omega_a^2}\right) \tag{4}$$

The nonlinear refractive index is estimated [38]:

$$n_2 = \frac{\Delta\phi}{KI_0L_{eff}} \tag{5}$$

where ($K = 2\pi/\lambda$), I_0 is the intensity of the laser beam at the focus point at $Z = 0$ (13.6 MW/m2), L_{eff} is the effective thickness of the sample, and it is based on the following equation:

$$L_{eff} = \frac{[1 - \exp(-\alpha L)]}{\alpha} \tag{6}$$

where L is the thickness of the sample and α is the linear absorption coefficient (247.04 cm-1). The peak valley pattern of the normalized transmittance curve is found under the closed aperture (CA), and the valley pattern of the normalized transmittance curve is found under the open aperture (OA) configuration (Figs. 10 and 11). The normalized open aperture curve for the samples produces the value of the nonlinear absorption coefficient. The nonlinear absorption coefficient (β) is estimated:
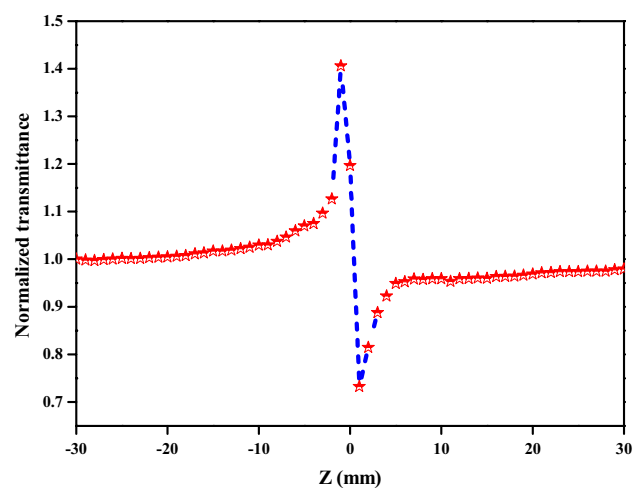

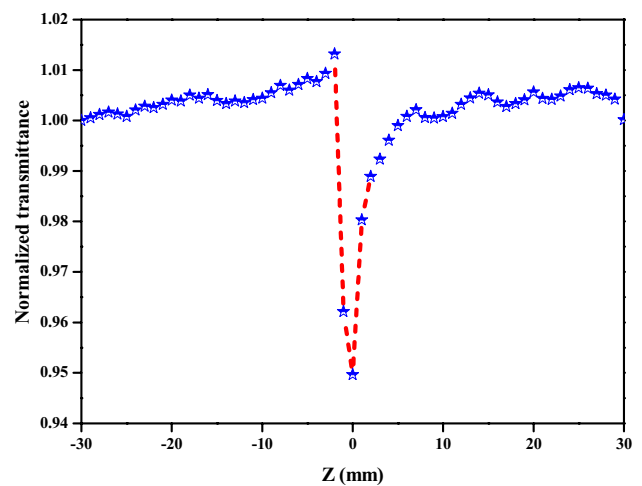**Fig. 10** Closed aperture curve of TPB single crystal

Fig. 11 Open aperture curve of TPB single crystal

$$\beta = \frac{2\sqrt{2}\Delta T}{I_0L_{eff}} \tag{7}$$

where ΔT is the open aperture curve value at one valley. The nonlinear absorption coefficient (β) revealed a positive value in the case of two-photon absorption and negative as saturable absorption. The real and imaginary parts of the third-order nonlinear optical susceptibility χ(3) are evaluated using the following expressions [39]:

$$\text{Re}\,\chi^{(3)} = \frac{10^{-4}(\varepsilon_0 C^2 n_0^2 n_2)}{\pi}\left(cm^2 W^{-1}\right) \tag{8}$$

$$\text{Im}\,\chi^{(3)} = \frac{10^{-2}(\varepsilon_0 C^2 n_0^2 \lambda\beta)}{4\pi^2}\left(cmW^{-1}\right) \tag{9}$$

where ε_0 indicates the vacuum permittivity $(8.854 \times 10^{-12}$ F/m), and n_0 is the linear refractive index. The refractive index of the TPB crystal was calculated from the prism coupling technique with a commercial prism coupler Metricon 2010/M (Metricon Corporation, UK) model at 532 nm in room temperature, and it was found to be 1.5338, laser wavelength (λ) of the beam is 532 nm, and C denotes the velocity of light in vacuum. The third-order nonlinear optical susceptibility of the TPB crystal can be found from the following expression:

$$\chi^{(3)} = \sqrt{\left(\mathrm{Re}\,\chi^{(3)}\right)^2 + \left(\mathrm{Im}\,\chi^{(3)}\right)^2} \qquad (10)$$

The second-order hyperpolarizability which reveals the nonlinear induced polarization per molecule is associated with the third-order susceptibility assessed by [40]:

$$\gamma_h = \frac{\chi^{(3)}}{f^4 N_*} \qquad (11)$$

where N^* is the density of the TPB molecule, calculated by the mentioned equation ($N^* = \rho NA/M$). The molar mass of the grown TPB compound is $M = 306.40$ g/mol, and NA is Avogadro's number $(6.023 \times 10^{23}$ mol^{-1}). The density of TPB crystal is 1.1990 g/cm^3. f is the local field factor according to Lorentz approximation given by:

$$f = \frac{\left(n_0^2 + 2\right)}{3} \qquad (12)$$

The relationship of the imaginary part (Im) $\chi^{(3)}$ to the real part (Re) $\chi^{(3)}$ is represented by the coupling factor (ρ^*) of third-order nonlinear susceptibility.

$$\rho^* = \frac{\mathrm{Im}\,\chi^{(3)}}{\mathrm{Re}\,\chi^{(3)}} \qquad (13)$$

The determined values of nonlinear parameters such as imaginary part Im $\chi^{(3)}$ and real part Re $\chi^{(3)}$ susceptibility are 2.9912×10^{-09} and 7.09459×10^{-10}, respectively. The coupling factor (ρ^*) is 0.2371, and third-order nonlinear susceptibility $\chi^{(3)}$ is 3.07422×10^{-09} esu. The nonlinear absorption can be attributed to the reverse saturation absorption process, while nonlinear refraction leads to a self-defocusing effect in the compound. The present work suggests that the TPB crystal possesses higher third-order nonlinear optical susceptibility ($\chi^{(3)}$) value compared with some of the NLO crystals and it is given in Table.1 [31, 41–43]. Hence, the above observations reveal that the grown TPB crystal can be used for nonlinear optical applications and optoelectronic device fabrications.

Table 1 Comparison of third-order nonlinear optical susceptibility $\chi^{(3)}$ value of TPB crystal with some previous reports (organic and inorganic NLO crystals)

S. no.	Crystals	$\chi^{(3)}$ (esu)	References
1	TPB	3.07422×10^{-09} esu	Present work
2	Imidazolium hydrogen maleate	5.764×10^{-09} esu	[41]
3	Sulfamic acid	5.004×10^{-10} esu	[42]
4	VMST	9.69×10^{-12} esu	[31]
5	LACC	0.9134×10^{-15} esu	[43]

4 Conclusion

Good-quality 1, 3, 5-triphenylbenzene (TPB) single crystal has been grown from solution by slow-cooling seed rotation technique. The UV–Visible analysis shows the grown crystal with good transparency in the entire visible region, which is an important aspect of scintillation and optical applications. The FWHM of grown TPB single crystal was 18 arcsec, and it indicated that the TPB crystal has good crystalline perfection. The luminescence analysis found the strong violet emission wavelength at 352 nm, which is due to the $\pi^*-\pi$ electron charge transition of the TPB crystal. The laser damage threshold value of the TPB crystal is 1.251 GW/cm^2. The Z-scan measurement revealed that the grown TPB crystal has a positive nonlinear absorption coefficient and third-order nonlinear optical susceptibility. Hence from the observations, it is concluded that the grown TPB crystal can be used for scintillation and optical applications.

References

1. C. Bosshard, J. Hulliger, M. Florsheimer, P. Gunter, *Organic nonlinear optical materials* (CRC Press, Boca Raton, 2001)
2. J. Zyss, *Molecular nonlinear optics: materials, physics, and devices* (Academic Press, Newyork, 2013)
3. D.S. Chemla (ed.), *Nonlinear optical properties of organic molecules and crystals*, vol. 1 (Elsevier, Amsterdam, 2012)
4. M. Shkir, A. Irfan, S. AlFaify, P.S. Patil, A.G. Al-Sehemi, Linear, second and third order nonlinear optical properties of novel noncentrosymmetric donor-acceptor configure chalcone derivatives: A dual approach study. Optik **199**, 163354 (2019)
5. S. Omar, M. Mohd Shkir, A. Khan, S. Zubair Ahmad, A. AlFaify, Comprehensive study on molecular geometry, optical, HOMO-LUMO, and nonlinear properties of 1, 3-diphenyl-2-propen-1-ones chalcone and its derivatives for optoelectronic applications: A computational approach. Optik **204**, 164172 (2020)
6. M. Ebrahimzadeh, A.I. Ferguson, Novel nonlinear crystals, in *Principles and Applications of Nonlinear Optical Materials*, ed.

by R.W. Munn, C.N. Ironside (Springer, Dordrecht, 1993), pp. 99–142

7. T. Sasaki, A. Yokotani, Growth of large KDP crystals for laser fusion experiments. J. Cryst. Growth **99**, 820–826 (1990)

8. P. Rajesh, S. Sreedhar, K. Boopathi, S.V. Rao, P. Ramasamy, Enhancement of the crystalline perfection of %3c 0 0 1%3e directed KDP single crystal. Curr. Appl. Phys. **11**, 1343–1348 (2011)

9. P.S. Patil, S.R. Maidur, J.R. Jahagirdar, T.S. Chia, C.K. Quah, M. Shkir, Crystal structure, spectroscopic analyses, linear and third-order nonlinear optical properties of anthracene-based chalcone derivative for visible laser protection. Appl. Phys. B **125**, 163 (2019)

10. G. Zhou, G. Li, Y. Lü, Y. Ma, X. Sun, X. Deng, P. Zhang, G. Lu, X. Wang, Growth and characterization of L-phenylalanine doped KDP crystals. Mater. Res. Bull. **113**, 146–151 (2019)

11. Z.S. Fadhul, E.A. Ali, S.R. Maidur, P.S. Patil, M. Shkir, F.Z. Henari, Thermally induced optical nonlinearity and optical power limiting action of 2, 4, 5-trimethoxy-4′-nitrochalcone under CW laser regime. J. Nonlinear Opt. Phy. Mater. **27**, 1850012 (2018)

12. G.F. Knoll, *Radiation Detection and Measurement* (John Wiley & Sons, Newyork, 2010)

13. N. Zaitseva, L. Carman, A. Glenn, J. Newby, M. Faust, S. Hamel, N. Cherepy, S. Payne, Application of solution techniques for rapid growth of organic crystals. J. Cryst. Growth **314**, 163–170 (2011)

14. M. Manikandan, P. Rajesh, P. Ramasamy, Crystal growth, structural, optical, vibrational analysis, Hirshfeld surface and quantum chemical calculations of 1, 3, 5-triphenylbenzene single crystal. J. Mol. Struct. **1195**, 659–669 (2019)

15. N. Durairaj, S. Kalainathan, M.V. Krishnaiah, Investigation on unidirectional growth of 1, 3, 5-Triphenylbenzene by Sankarana-rayanan–Ramasamy method and its characterization of lifetime, thermal analysis, hardness and etching studies. Mater. Chem. Phys. **181**, 529–537 (2016)

16. P. Karuppasamy, T. Kamalesh, M.S. Pandian, P. Ramasamy, S. Verma, Growth of high- quality organic single crystal of 2-ami-nopyridinium 4-nitrophenolate 4-nitrophenol (2AP4N) by a novel Rotational Sankaranarayanan–Ramasamy (RSR) method. J. Cryst. Growth **518**, 59–72 (2019)

17. M. Shkir, P.S. Patil, M. Arora, S. AlFaify, H. Algarni, An experimental and theoretical study on a novel donor-π-acceptor bridge type 2, 4, 5-trimethoxy-4′-chlorochalcone for optoelectronic applications: a dual approach. Spectrochim. Acta, Part A **173**, 445–456 (2017)

18. G. Socrates, *Infrared and Raman Characteristic Group Frequencies: Tables and Charts* (John Wiley & Sons, Newyork, 2004)

19. J. Coates, Interpretation of infrared spectra, a practical approach. In: *Encyclopedia of analytical chemistry: applications, theory and instrumentation* (Wiley, 2006)

20. G. Keresztury, J.M. Chalmers, P.R. Griffith, *Raman Spectroscopy: Theory in Handbook of Vibrational Spectroscopy* (John Wiley & Sons Ltd., New York, 2002)

21. J.H.S. Green, D.J. Harrison, W. Kynaston, Vibrational spectra of benzene derivatives—XI 1, 3, 5-and 1, 2, 3-trisubstituted compounds. Spectrochim. Acta, Part A **27**, 793–806 (1971)

22. J. Liu, F. You, C. Hu, Y. Ma, F. Teng, T. Wang, J. Tang, L. Cao, B. Teng, Growth and characterization of organic 4-chloroben-zaldehyde-N-methyl 4 stilbazoliumtosylate crystal: A promising material for nonlinear optical device applications. Optik **178**, 999–1009 (2019)

23. R. Subramaniyan@ Raja, G. Anandha Babu, P. Ramasamy, Studies on the growth and characterization of an organic single crystal–1, 3, 5-Triphenylbenzene. Mater. Res. Innov. **22**, 1–6 (2018)

24. L.G. Prasad, V. Krishnakumar, R. Nagalakshmi, S. Manohar, Physicochemical properties of highly efficient organic NLO crystal: 4-Aminobenzamide. Mater. Chem. Phys. **128**, 90–95 (2011)

25. G. Hull, N.P. Zaitseva, N.J. Cherepy, J.R. Newby, W. Stoeffl, S.A. Payne, New organic crystals for pulse shape discrimination. IEEE Trans. Nucl. Sci. **56**, 899–903 (2009)

26. G. Bhagavannarayana, R.V. Ananthamurthy, G.C. Budakoti, B. Kumar, K.S. Bartwal, A study of the effect of annealing on Fe-doped LiNbO3 by HRXRD, XRT and FT–IRJ. Appl. Crystallogr. **38**, 768–771 (2005)

27. B.W. Batterman, H. Cole, Dynamical diffraction of x rays by perfect crystals. Rev. Mod. Phys. **36**, 681 (1964)

28. N.L. Boling, M.D. Crisp, G. Dube, Laser induced surface damage. Appl. Opt. **12**, 650–660 (1973)

29. S.K. Sharma, S. Verma, Y. Singh, K.S. Bartwal, M.K. Tiwari, G.S. Lodha, G. Bhagavannarayana, Investigations of structural defects, crystalline perfection, metallic impurity concentration and optical quality of flat-top KDP crystal. Opt. Mater. **46**, 329–338 (2015)

30. R.M. Jauhar, V. Viswanathan, P. Vivek, G. Vinitha, D. Velmurugan, P. Murugakoothan, A new organic NLO material isonicoti-namidium picrate (ISPA): crystal structure, structural modeling and its physico-chemical properties. RSC Adv. **6**, 57977–57985 (2016)

31. M.K. Kumar, S. Sudhahar, P. Pandi, G. Bhagavannarayana, R.M. Kumar, Studies of the structural and third-order nonlinear optical properties of solution grown 4-hydroxy-3-methoxy-4′-N′-methylstilbazolium tosylate monohydrate crystals. Opt. Mater. **36**, 988–995 (2014)

32. N. Vijayan, G. Bhagavannarayana, R. Ramesh Babu, R. Gopalakrishnan, K.K. Maurya, P. Ramasamy, A comparative study on solution-and bridgman-grown single crystals of benzimidazole by high-resolution X-ray diffractometry, fourier transform infrared, microhardness, laser damage threshold, and second-harmonic generation measurements. Cryst. Growth Design **6**, 1542–1546 (2006)

33. M. Sheik-Bahae, A.A. Said, T.H. Wei, D.J. Hagan, E.W. Van Stryland, Sensitive measurement of optical nonlinearities using a single beam. IEEE J. Quantum Electron. **26**, 760–769 (1990)

34. R. DeSalvo, M. Sheik-Bahae, A.A. Said, D.J. Hagan, E.W. Van Stryland, Z-scan measurements of the anisotropy of nonlinear refraction and absorption in crystals. Opt. Lett. **18**, 194–196 (1993)

35. D. Sajan, N. Vijayan, K. Safakath, R. Philip, I.H. Joe, Intramolecular charge transfer and Z-scan studies of a semiorganic nonlinear optical material sodium acid phthalate hemihydrate: a vibrational spectroscopic study. J. Phys. Chem. A **115**, 8216–8226 (2011)

36. M. Shkir, M. Anis, S. Shaikh, S. AlFaify, An investigation on structural, morphological, optical and third order nonlinear properties of facilely spray pyrolysis fabricated In: CdS thin films. Superlattices Microstruct. **133**, 106202 (2019)

37. M. Shkir, M. Anis, S. Shafik, M.A. Manthrammel, M.A. Sayeed, M.S. Hamdy, S. AlFaify, An effect of Zn content doping on opto-third order nonlinear characteristics of nanostructured CdS thin films fabricated through spray pyrolysis for optoelectronics. Phys. E: Low-dimensional Syst. Nanostruct. **118**, 113955 (2020)

38. Y.S. Liu, Spectral phase-matching properties for second-harmonic generation in nonlinear crystals. Appl. Phys. Lett. **31**, 187–189 (1977)

39. P. Karuppasamy, V. Sivasubramani, M.S. Pandian, P. Ramasamy, Growth and characterization of semi-organic third order nonlinear optical (NLO) potassium 3, 5-dinitrobenzoate (KDNB) single crystals. RSC Adv. **6**, 109105–109123 (2016)

40. M.T. Zhao, B.P. Singh, P.N. Prasad, J. Chem. Phys. **89**, 5535–5541 (1988)

41. K. Elangovan, A. Senthil, Growth, structural, spectral, thermal, mechanical, electrical, linear and third order nonlinear optical properties of Imidazolium hydrogen maleate (IM) single crystal for nonlinear optical applications. Mater. Res. Express **6**, 065101 (2019)

42. J. Arumugam, M. Selvapandiyan, S. Chandran, M. Srinivasan, P. Ramasamy, Crystal growth, optical, thermal, laser damage threshold, photoconductivity and third-order nonlinear optical studies of KCl doped sulphamic acid single crystals. J. Mater. Sci. Mater. Electron. **31**, 6084–6096 (2020)

43. P. Kalaiselvi, S.A.C. Raj, N. Vijayan, Linear and nonlinear optical properties of semiorganic single crystal: l-Alanine cadmium chloride (LACC). Optik **124**, 6978–6982 (2013)